

激光-电弧复合焊接 7075-T6 铝合金疲劳断裂特性

吴圣川^{1,2}, 徐晓波¹, 张卫华², 李 正¹, 徐道荣¹

(1. 合肥工业大学 材料科学与工程学院, 合肥 230009;

2. 西南交通大学 牵引动力国家重点实验室, 成都 610031)

摘 要: 研究激光-电弧复合焊接 2 mm 板 7075-T6 铝合金在不同应力比 R 和应力幅 σ_a 下的疲劳裂纹扩展行为。结果表明, 优选的复合焊工艺参数激光功率 3 kW、电流 110 A 和焊接速度 3 m/min 条件下接头和母材的疲劳裂纹扩展速率曲线存在交叉现象, 即当应力强度因子幅 ΔK 小于 $15.6 \text{ MPa} \cdot \text{m}^{1/2}$ 时, 接头的疲劳裂纹扩展速率小于母材, 反之则接头的疲劳裂纹扩展速率大于母材。而对应同一 ΔK 值, 高应力比下的疲劳裂纹扩展速率快于低应力比条件下的扩展速率。应力幅或平均应力是影响疲劳裂纹扩展特性的主要因素。

关键词: 激光-电弧复合焊; 7075 高强铝合金; 疲劳断裂; 微观组织; 软化效应

中图分类号: TG456.7 文献标识码: A 文章编号: 0253-360X(2012)10-0045-04



吴圣川

0 序 言

近年来, 运载工具的“轻量化”引起各国重视, 高强铝合金以优异的综合力学性能成为重要的优选结构材料。激光-电弧复合焊是当前最具发展潜力的轻合金熔焊技术, 在高速列车结构制造中具有广阔的发展应用前景^[1,2]。然而在复杂的服役载荷下, 熔焊缺陷如裂纹和气孔的缺口效应持续增强并发展, 导致关键结构部件的失效, 成为高速列车运营的重大安全隐患^[3,4]。疲劳裂纹扩展速率是损伤容限设计的主要性能指标^[5], 迄今仍少见激光-电弧复合焊 7075-T6 铝合金接头疲劳特性的研究。

文中通过母材与接头的疲劳裂纹扩展速率、断口形貌、组织观察以及显微硬度等来深入研究高强铝合金熔焊 7075-T6 接头和母材的疲劳断裂性能, 为结构设计与工程应用提供技术支持。

1 试验方法

材料为 2 mm 厚 T6 态的 7075 铝合金轧制板材。填充焊丝型号为 ER5356, 直径 1.2 mm。拉伸试验获得的力学性能为: 接头屈服强度 $R_{eL} = 210$

MPa, 抗拉强度 $R_m = 280 \text{ MPa}$; 母材屈服强度 $R'_{eL} = 437 \text{ MPa}$, 抗拉强度 $R'_m = 525 \text{ MPa}$ 。

由接头和母材的拉伸试验可知, 接头的屈服强度约为母材的 48%, 抗拉强度是母材的 53%。再由熔焊接头失配度 $M = \text{接头 } R_{eL} / \text{母材 } R'_{eL}$, 可知 7075-T6 铝合金激光-电弧复合焊接头的 $M < 1$, 属于低匹配。然而, 焊接接头的疲劳性能并不能简单的根据强度大小来判断, 已有大量的研究表明, 铝合金的裂纹扩展速率受强度的影响并不明显。

在光纤激光-电弧复合焊平台上对接焊, 优化的焊接参数为: 激光功率 $P = 3 \text{ kW}$, 电流 $I = 110 \text{ A}$, 焊接速度 $v = 3 \text{ m/min}$, 送丝速度 $v_1 = 5.3 \text{ m/min}$, 离焦量 -1 mm , 氩气流量为 150 L/min 。此外, 为防止铝合金表面反射出的激光对光纤的损伤, 激光束偏移试板的法向约 10° , 电弧偏移法线约 20° 。依照国家标准 GB/T 6398—2000《金属材料疲劳裂纹扩展速率试验方法》制取紧凑拉伸 (CT) 试样。先用粗砂纸磨去焊缝背面的毛刺, 再用细砂纸将试样表面磨至平整光亮, 以消除几何不平整的影响。

在 MTS-809 型电液伺服材料试验机上预制裂纹, 然后施加正弦恒幅载荷。试验载荷频率 $f = 10 \text{ Hz}$, 以峰值载荷 $P_{\max} = 1600 \text{ N}$ 作为预制裂纹峰值载荷并连续逐级卸载至真实试验载荷 1200 N , 预制裂纹长度 1.5 mm 以上即可。试验条件为室温和大气环境, 裂纹长度采用 10 倍放大镜监测, 用目测法测量, 每隔 0.5 mm 读一次循环周次。母材和接头疲劳

收稿日期: 2011-08-10

基金项目: 国家自然科学基金资助项目 (51005068); 牵引动力国家重点实验室自主课题资助项目 (2012TPL-T18); 汽车车身先进设计制造国家重点实验室开放基金资助项目 (31115030)

断口形貌观察在 JSM-6490LV 型扫描电镜上进行。

2 试验结果与分析

由复合焊缝 CT 断口形貌可知,裂纹沿焊缝中心垂直于荷载方向扩展,只是随着裂纹的扩展裂纹面稍稍地偏转了一个角度。

2.1 疲劳裂纹扩展速率

图 1 为接头的疲劳裂纹扩展速率 da/dN 随裂纹长度的关系曲线。可见,在约 2/3 的寿命区内, da/dN 变化不明显。而在剩余 1/3 寿命区(以 $\Delta a = 9$ mm 为临界点)中, da/dN 明显加快,表明材料抵抗疲劳裂纹扩展的内在抗力大幅降低。

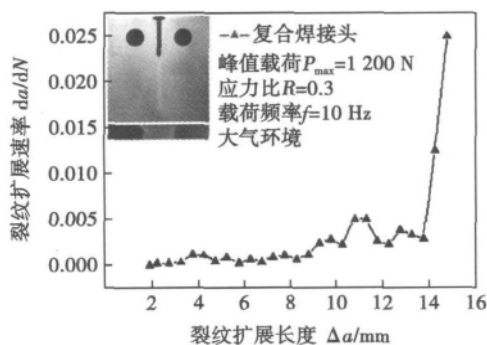


图 1 复合焊接头裂纹扩展速率与裂纹扩展长度的关系
Fig. 1 Relationship between crack growth rate and crack-extension of welded joint

裂纹稳定扩展阶段(即疲劳裂纹扩展第 II 阶段)是焊接接头的主要寿命区间,对应的应力强度因子幅 ΔK 较大($\Delta K_{th} < \Delta K \ll \Delta K_c$)。此外, da/dN 正比于应力强度因子幅 ΔK ,在对数坐标下, da/dN 和 ΔK 的关系为一直线^[6]。将稳定扩展阶段的 da/dN 和 ΔK 分别取对数,绘制在以 $\lg(da/dN)$ 为纵轴、 $\lg(\Delta K)$ 为横轴的双对数坐标图上,见图 2。

由图 2 看出,母材和接头在同样加载条件下的疲劳裂纹扩展速率曲线存在交叉现象。在低于应力强度因子幅约 $15.6 \text{ MPa} \cdot \text{m}^{1/2}$ 时,接头的裂纹扩展速率慢于母材;反之则快于母材,表明焊缝为结构的危险区域。试验表明,当对接头施加的载荷使焊缝处裂纹尖端的 $\Delta K \leq 15.6 \text{ MPa} \cdot \text{m}^{1/2}$ 时,接头断裂性能优于母材,否则接头将面临失稳断裂危险。实际服役过程中,应注意并合理调整焊缝布置、结构设计和极限荷载,以避免灾难性事故发生。

用最小二乘法线性回归得到疲劳裂纹参数。则由 $da/dN = C(\Delta K)^n$,且应力比 $R = 0.3$ 时: $C = 3.445 \times 10^{-14}$, $n = 6.022$;而母材在 $R = 0.3$ 和 0.1

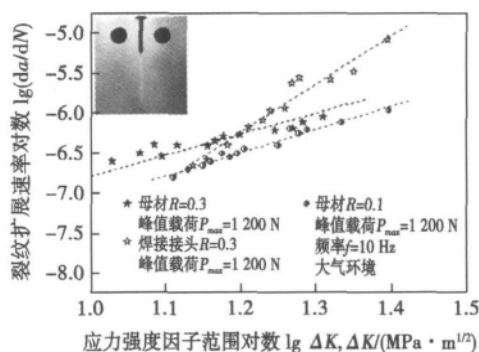


图 2 母材及复合焊接头的 $\lg(da/dN) - \lg(\Delta K)$ 关系
Fig. 2 Relationships between crack growth rate and SIF range for hybrid welded joint and base metal

时, $C = 4.002 \times 10^{-10}$, $n = 2.615$ 与 $C = 1.071 \times 10^{-10}$, $n = 2.902$ 。

对比分析 $R = 0.1$ 和 0.3 下母材的裂纹扩展行为,发现对同一 ΔK 值 $R = 0.3$ 时的裂纹扩展速率快于 $R = 0.1$ 。由 Forman 公式 $da/dN = C(\Delta K)^n / [(1-R)K_c - \Delta K]$ 可知,在相同 ΔK 值下,随着 R 增加,裂纹扩展加快。其实质是裂纹顶端往后所遗留的塑变“尾迹”效应。当最大峰值应力 σ_{max} 卸载到最小应力 σ_{min} 时,裂尖材料从卸载初期尚有少量的残余拉应力过渡进入压缩状态,最终使裂尖区产生残余压应力。当下一个拉伸循环开始时,裂尖处拉应力须先克服上个循环结束时所产生的压应力,然后才可使裂纹继续张开并向前扩展,实际上控制材料裂纹扩展特性的是裂尖的有效应力强度因子 ΔK_{eff} 。由于闭合效应会降低裂纹尖端的局部扩展驱动力,而高的应力比(或平均应力)不利于裂纹闭合,会加速疲劳裂纹的扩展,所以 $R = 0.3$ 时的疲劳裂纹扩展速率位于在 $R = 0.1$ 时曲线上方。

表 1 为母材在初始裂纹长度 a_0 、峰值载荷 P_{max} 、载荷幅 ΔP , $R = 0.1$ 和 0.3 的寿命数据。结果表明,应力幅对材料的疲劳寿命影响比应力比 R 大。

表 1 同一峰值载荷不同应力比下母材的疲劳数据
Table 1 Fatigue parameters under different conditions

应力比	峰值载荷	载荷幅	裂纹扩展长度	循环周次
R	P_{max}/N	$\Delta P/N$	a_0/mm	$N/周$
0.1	1 200	1 080	19.3	27 019
0.3	1 200	840	18.7	43 845

2.2 疲劳断口形貌

图 3 和图 4 分别为母材和接头在 $P_{max} = 1 200$ N, $R = 0.3$ 时的疲劳断口形貌。其中图 3a、b 为裂纹扩展的稳定阶段,在图 3a 中可看到较多塑性疲劳条

带(如椭圆标示),也有少量脆性疲劳条带,整体看上去又似羽毛状结构。从图 3b 中可清楚看到疲劳条带,它是裂纹扩展时留下的微观痕迹,是一系列基本上相互平行的条纹,条带方向与局部裂纹扩展方

向垂直并且条纹沿着局部裂纹扩展方向向外凸。母材瞬断区断口形貌与静载拉伸断口类似,特征是呈现较浅的等轴韧窝和拉长韧窝,如图 3c 所示。

图 4a, b 分别为稳定扩展阶段的气孔和疲劳

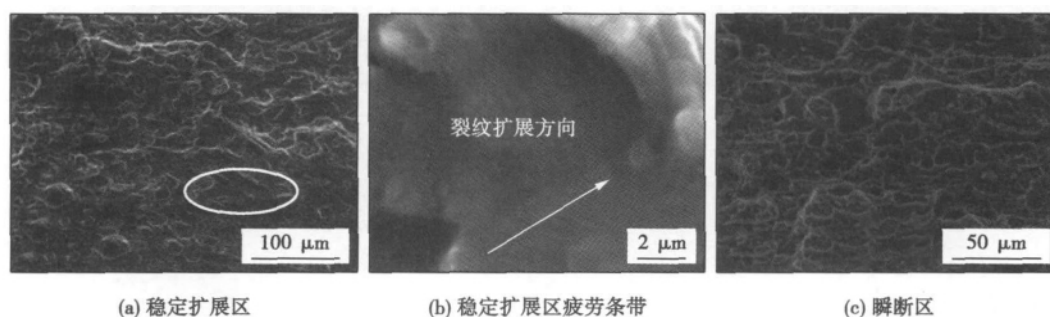


图 3 应力比 $R=0.3$ 下母材的疲劳断口形貌

Fig. 3 Fatigue fracture appearance of base metal when $R=0.3$

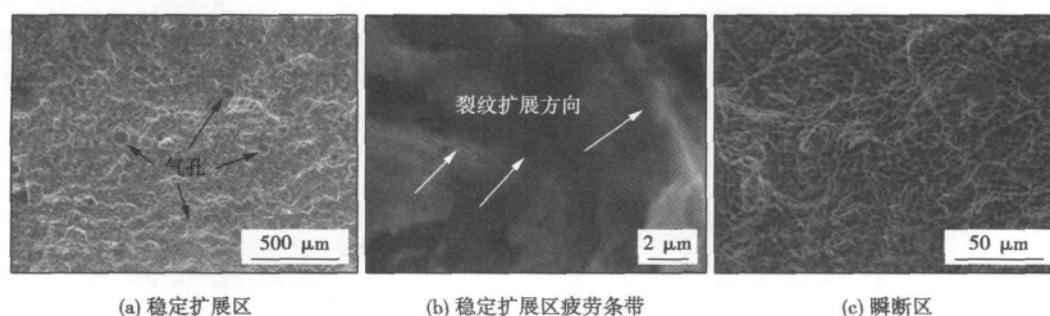


图 4 应力比 $R=0.3$ 下复合焊接头的疲劳断口形貌

Fig. 4 Fatigue fracture appearance of hybrid welded joint when $R=0.3$

条带,可见与母材的扩展形貌明显不同。图 4a 中有大小不一、密集分布的气孔,这些气孔往往成为疲劳裂纹萌生源,是导致接头承载能力下降的原因之一。图 4b 是不同平面上的疲劳条带,表明焊后材料内组织和应力状态差异较大,从而导致应力循环时裂纹由一个平面攀移至另一个平面,并最终影响 da/dN 的大小。图 4c 为瞬断区形貌,可观察到大量的韧窝,与静载拉伸断口类似。

2.3 显微组织

复合焊接头的显微组织如图 5 所示。图 5a 为熔合区(FZ)的组织形貌,可以清楚看出,熔合区晶粒尺寸较小,具有典型的铸造组织特征。图 5b 为部分熔合区(PMZ),该区的晶粒亦较小,呈现出柱状晶特征,并指向焊缝中心,其生长具有强烈的方向性。5c 为焊缝热影响区(HAZ),该区晶粒较熔合区的粗大,并且晶粒大小不均匀。由于焊缝晶粒较细,晶界较多,可以有效提高接头的滑移形变抗力,能极大地影响短裂纹的扩展,而通常晶界对长裂纹的扩

展只有很小的影响。

2.4 显微硬度

接头横截面上的硬度分布如图 6 所示。可见,硬度在各区的分布很不均匀,熔合区硬度最低,约为母材硬度 60%,热影响区硬度可达母材的 90% 以上,且热影响区的宽度接近焊缝,表明激光-电弧复合焊接 7075-T6 铝合金接头中存在着严重的软化现象。这种软化效应是热循环致母材强化效果部分消失和非热处理强化填充金属加入的综合效应。

3 讨 论

激光-电弧复合焊接 7075-T6 铝合金接头和母材的疲劳裂纹扩展速率曲线存在交叉现象,这正说明了接头的疲劳裂纹扩展行为受多因素影响。这些因素对裂纹的扩展作用并非步调一致,且在扩展的不同阶段其作用程度不同。由于铝合金的裂纹扩展速率受强度影响很小,且长裂纹的扩展对晶粒尺寸

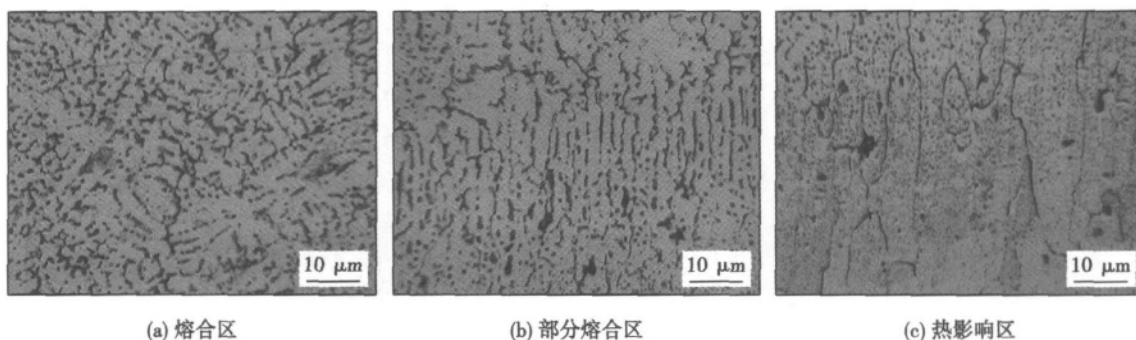


图 5 复合焊接 7075-T6 铝合金接头显微组织

Fig. 5 Microstructures of hybrid welded 7075-T6 joint

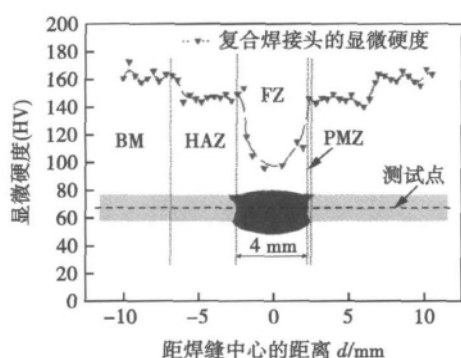


图 6 复合焊接 7075-T6 铝合金接头硬度分布

Fig. 6 Hardness distribution of hybrid welded 7075-T6 joint

变化不敏感^[6]。结合图 6 中复合焊接头的软化现象以及 Head 曾提出的包含裂纹尖端塑性区尺寸的裂纹扩展模型,对结果中出现的交叉现象加以解释。式(1)为 Head 扩展模型。

$$\frac{da}{dN} = \frac{C_1 \Delta \sigma a^{3/2}}{(C_2 - \sigma) \omega_0^{1/2}} \quad (1)$$

式中: $\Delta \sigma$ 是应力幅值; ω_0 是裂纹尖端塑性区尺寸, C_1, C_2 为常数。显然,由于熔焊接头的软化效应,导致相同条件下裂纹尖端塑性区尺寸较母材的大。由式(1)可知,单独考虑裂纹尖端塑性区尺寸时接头的裂纹扩展速率将小于母材。

4 结 论

(1) 激光-电弧复合焊接头的裂纹扩展速率为: $da/dN = 3.4 \times 10^{-14} (\Delta K)^{6.022} (R = 0.3)$, 母材在应力比 $R = 0.3$ 和 0.1 时分别为: $da/dN = 4.0 \times 10^{-10} (\Delta K)^{2.615}$ 和 $da/dN = 1.1 \times 10^{-10} (\Delta K)^{2.902}$ 。

(2) 接头和母材的 da/dN 曲线有交叉现象,当 $\Delta K \leq 15.6 \text{ MPa} \cdot \text{m}^{1/2}$ 时,接头的疲劳裂纹扩展速率小于母材,表明该熔焊接头可以安全服役。

(3) 同一 ΔK 值条件下,高应力比下的疲劳裂纹扩展速率快于低应力比条件下的扩展速率。

(4) 应力幅或平均应力是影响疲劳裂纹扩展速率的主要因素,其次才是应力比。

必须指出,影响熔焊接头 da/dN 的因素较多,机理复杂。采用粗略的目测法记录 Δa 是误差源之一。此外熔焊气孔对 da/dN 的影响应成为研究车体关键接头超高周疲劳损伤的重要内容。

参考文献:

- [1] 杨 璟,李晓延,巩水利,等. 铝锂合金 YG-MIG 复合焊焊接成形特征[J]. 焊接学报,2010,31(2): 83-86.
Yang Jing, Li Xiaoyan, Gong Shuili, et al. Characteristics of aluminium-lithium alloy joint formed by YAG-MIG hybrid welding [J]. Transactions of the China Welding Institution, 2010, 31(2): 83-86.
- [2] 王炎金. 铝合金车体焊接工艺[M]. 北京: 机械工业出版社, 2011.
- [3] 钟群鹏,赵子华. 断口学[M]. 北京: 高等教育出版社,2006.
- [4] 王希靖,李树伟,牛 勇,等. A7075 搅拌摩擦焊疲劳裂纹扩展速率试验分析[J]. 焊接学报,2008,29(9): 5-7.
Wang Xijing, Li Shuwei, Niuyong, et al. Fatigue crack growth rate of A7075 FSW [J]. Transactions of the China Welding Institution, 2008, 29(9): 5-7.
- [5] 蹇海根,姜 锋,郑秀媛,等. 采用 EBSD 研究高强铝合金的疲劳裂纹扩展行为[J]. 材料热处理学报,2011,32(2): 75-80.
Jian Haigen, Jiang Feng, Zheng Xiuyuan, et al. EBSD analysis of propagation behavior of fatigue cracks in high strength aluminum alloy [J]. Transactions of Materials and Heat Treatment, 2011, 32(2): 75-80.
- [6] Pearson S. Fatigue crack propagation in metals [J]. Nature, 1966, 211: 1077-1078.

作者简介: 吴圣川,男,1979 年出生,副研究员。主要从事高速列车结构疲劳可靠性及其仿真软件开发等方面的工作。发表论文 30 余篇。Email: wusc@home.swjtu.edu.cn

fect of HT250 castiron used in diesel engine cylinder was repaired with inferior-laser instantaneous melting cold-welding technology. The cold-welding residual stress was measured through the X-ray diffraction method to study the regularity of residual stress and the relationship between the residual stress and different process parameters. The results show that the stress near the weld seam is tensile and the stress away from the weld seam is compressive. The cold welding residual stress distribution is quite narrow. The peak stress mainly distributes in the range of 5mm from the weld seam center and the residual stress is close to zero in the place of 20 mm away from the weld seam center. Time parameter has little influence on the peak stress while the energy parameter's influence is great. Through the change of time and energy , smaller residual peak stress can be obtained to meet the repair requirements for surface damage on engine remanufacturing parts.

Key words: cold-welding; surface residual stress; process parameters; remanufacturing

Pitting corrosion resistance of PH stainless steel of FV520B and its welding joint

ZHANG Min¹ ,ZHANG Enhua¹ ,ZHI Jinhua^{1,2} , MENG Qiang¹ ,ZHANG Haicun² (1. School of Material Science and Engineering , Xi'an University of Technology , Xi'an 710048 , China; 2. Xi'an Shangu Power Co. ,Ltd , Xi'an 710075 , China) . pp 37 -40

Abstract: The corrosion-resistance of the steel FV520B had been tested respectively in the HCl and H₂SO₄ (10%) under the 35 °C . The result showed that under the above condition the base metal and the welding joint suffered a much more serious pitting corrosion in the HCl (10%) than that in the H₂SO₄ of the same mass fraction ,the chloridion has more serious destructive effect on the passivation film of the stainless steel , which causes the deeper corrosive pitting. while the corrosive effect of 10% mass fraction H₂SO₄ is relatively inferior ,the corrosion products are different either ,but under the different corrosive environment ,all the corrosive level of the weld joint in the welding point is lower than the HAZ.

Key words: precipitation sclerosis stainless steel; microstructure; corrosion resistance

Interfacial microstructure and properties of Si₃N₄ joints brazed using TiNi-V eutectic brazing alloy

WANG Guoxing¹ , SONG Xiaoguo^{2,3} , CHEN Haiyan³ , LI Yang¹ , CAO Jian^{2,3} (1. School of Materials & Chemical Engineering , Heilongjiang Institute of Technology , Harbin 150050 , China; 2. School of Materials Science & Engineering , Harbin Institute of Technology at Weihai , Weihai 264209 , China; 3. State Key Lab of Advanced Welding and Joining , Harbin Institute of Technology , Harbin 150001 , China) . pp 41 -44

Abstract: TiNi-V eutectic brazing alloy was fabricated by vacuum arc melting ,and its spreadability on the surface of Si₃N₄ ceramic was investigated. The brazing of Si₃N₄ ceramic was achieved using TiNi-V brazing alloy. The typical interfacial microstructure was Si₃N₄/TiN + Ti-Si compounds/NiV. The effect of brazing temperature on the interfacial microstructure and properties of joints was investigated. The results showed that with the

increasing of brazing temperature , the reaction between molten brazing alloy and Si₃N₄ ceramic intensified and the thickness of TiN + Ti-Si compounds layer increased gradually. Moreover , lots of microcracks were formed in the joints due to the residual stress in joints , which deteriorated the joining properties. The highest shear strength of 28 MPa was obtained when the specimen was brazed at 1 200 °C for 10 min. The joint fractured in TiN + Ti-Si compounds layer , which belonged to brittle fracture.

Key words: TiNi-V eutectic brazing alloy; brazing; Si₃N₄ ceramic; interfacial microstructure

Fatigue fracture behavior of laser-MIG hybrid welded 7075-T6 aluminium alloys

WU Shengchuan^{1,2} , XU Xiaobo¹ , ZHANG Weihua² , LI Zheng¹ , XU Daorong¹ (1. School of Materials Science and Engineering , Hefei University of Technology , Hefei 230009 , China; 2. State Key Laboratory of Traction Power , Southwest Jiaotong University , Chengdu 610031 , China) . pp 45 -48

Abstract: The influence of stress ratio R and stress range σ_a on the fatigue crack propagation behavior of high strength 7075-T6 aluminum alloy and laser-MIG hybrid welded joint is studied. The results show that under the welding parameters of $P = 3\ 000\ \text{W}$, $I = 110\ \text{A}$ and $v = 3\ \text{m/min}$, the fatigue cracking growth rate curve of laser-arc hybrid welding joint intersects with that of base metal. That is due to that the fatigue crack growth rate of hybrid welding joint is lower than that of base metal especially when the SIF range ΔK is less than $15.6\ \text{MPa} \cdot \text{m}^{1/2}$. Under the conditions of same SIF range ΔK , the fatigue cracking growth rate at the higher stress ratio is larger than that of the lower stress ratio. Furthermore , the stress range is more important than the stress ratio (mean stress) to determine the fatigue cracking growth rate of welding joints.

Key words: hybrid laser-arc welding; 7075 high strength aluminium alloy; fatigue fracture; microstructure; softening effect

Arc stability of underwater wet flux-cored arc welding

SHI Yonghua , ZHENG Zepei , HUANG Jin (School of Mechanical and Automotive Engineering , South China University of Technology , Guangzhou 510640 , China) . pp 49 -53

Abstract: Standard deviation (SD) and the reciprocal of coefficient of variation (CV) of welding voltage are used as the index of arc stability. The arc stability of underwater wet flux-cored arc welding in different welding conditions was studied based on underwater wet welding experiments. Sensitivity models of arc stability have been built and sensitivities of welding parameters on arc stability , such as welding current , voltage , speed and water depth , were analyzed. The results showed that the arc stability got worse as water depth increased. Especially in shallow water , the arc stability decreased dramatically as the water depth increased. Arc stability also decreases with the increasing of welding speed. The welding voltage has a great influence on arc stability and increasing the welding voltage appropriately will improve the arc stability.

Key words: underwater welding; arc stability; sensitivity analysis